

Width of resonance Raman enhancement profiles in Cu_2O : The phonon-lifetime contribution

R. M. Habiger and A. Compaan

Department of Physics, Kansas State University, Manhattan, Kansas 66506

(Received 17 April 1978)

Near an isolated electronic resonance at ω_e the enhancement profile of the Raman intensity displays an "in" resonance for $\omega_L = \omega_e$, and an "out" resonance for $\omega_s = \omega_L - \omega_0 = \omega_e$, where ω_s , ω_L , and ω_0 are the scattered phonon, laser, and phonon frequencies, respectively. We demonstrate, with laser frequencies near the 1S yellow exciton in Cu_2O , that the shape of the Raman cross section versus frequency for the "in" resonance reflects the lifetime broadening of the exciton state. However, the shape of the "out" resonance is fit only by including both the electronic-state damping and the phonon damping.

The frequency dependence of the Raman cross section near an isolated electronic state displays in general two resonances.^{1,2} The first occurs when the incoming (laser) frequency is near resonance with the electronic state, the "in" resonance. The second arises when the Raman-shifted photon is near resonance with the electronic state, the "out" resonance. It has been shown that if the damping γ_e of this electronic state is much less than the phonon frequency ω_0 , then the Raman cross section for the in resonance case accurately reflects the absorption line shape of the electronic state.³ This behavior has been demonstrated for the case of the 1S yellow exciton in Cu_2O using quadrupole-dipole Raman scattering.⁴ The case of the out resonance is quite similar and may be treated in a nearly analogous way. However, careful consideration shows that the resonance width of the Raman cross section should reflect the phonon lifetime as well as the electronic-state lifetime.¹ In this paper we confirm this conclusion by comparing the in resonance and out resonance widths of Raman enhancements near the zero-phonon line of the 1S yellow exciton in Cu_2O . We find that the

difference in widths corresponds well with the phonon damping as obtained from a high-resolution (Fabry-Perot) determination of the intrinsic width of the first-order Raman line.

Single-phonon Raman scattering at optical frequencies is described well in terms of the golden rule in which three zeroth-order systems—the radiation field, the electrons (or excitons), and the nuclei—interact via the electron-radiation field interaction H_{e-R} and the electron-phonon (or electron-nuclear) interaction H_{e-N} . The zeroth-order states of the matter system are described, for this adiabatic approximation, in terms of product wave functions of the electronic or excitonic states and the phonon (vibrational) states. The typical matter state at zero temperature consists of an electronic state of energy $\hbar\omega_e^0$ with a phonon of frequency ω_0 present and shall be written $|i, \omega_0\rangle$; without the phonon it shall be written $|i, 0\rangle$. The overall matrix element describing single-phonon Stokes Raman scattering is then described in terms of third-order perturbation theory in which the most strongly resonant of six possible contributing terms is¹

$$K = \sum_{i,j} \langle g, \omega_0 | H_{e-R} | j, \omega_0 \rangle \langle j, \omega_0 | H_{e-N} | i, 0 \rangle \langle i, 0 | H_{e-R} | g, 0 \rangle / (\omega_j^e + \omega_0 - \omega_L + i\gamma_j) (\omega_i^e - \omega_L + i\gamma_i) \quad (1)$$

where $|g\rangle$ is the ground electronic state, $|i\rangle$ and $|j\rangle$ are the intermediate electronic states, and ω_L is the incident laser frequency. For describing the resonance behavior of the Raman cross section, the matrix elements are generally taken to be frequency independent and the frequency dependence is given solely by the resonant denominators. In order to describe situations very near resonance, the phenomenological damping terms γ_i and γ_j are introduced to describe the finite

lifetime of the intermediate states. Since the scattered photon frequency in Stokes scattering is $\omega_s = \omega_L - \omega_0$ the denominator on the left is often rewritten

$$(\omega_j^e + \omega_0 - \omega_L + i\gamma_j)^{-1} = (\omega_j^e - \omega_s + i\gamma_j)^{-1}. \quad (2)$$

This rearrangement of terms motivates the use of the phrase out resonance for the case when $\omega_j^e - \omega_s \approx \gamma_j$.

The damping terms γ_i and γ_j have usually received little direct attention since the effects of finite linewidth are often masked by multiple resonances or overlapping electronic states. However, it is in the convenient rearrangement of Eq. (2) to show explicitly the scattered photon resonance that particular care must be exercised with the damping terms. The damping parameter γ_j describes the complete damping of the full matter state $|j, \omega_0\rangle$ which therefore includes both the damping of the electronic state γ^e and of the phonon or vibrational state γ_0 , and thus $\gamma_j = \gamma_j^e + \gamma_0$.

In order to illustrate these effects for the case of an isolated exciton state in Cu_2O , we rewrite Eq. (1). In a region where a single electronic state of energy $\hbar\omega_a^e$ dominates the spectrum the double sum over i and j collapses to two terms with a single sum. Thus

$$K \sim \frac{1}{(\omega_a^e - \omega_L + i\gamma_a^e)} \sum_j \frac{M_j}{\omega_j^e - \omega_s + i\gamma_j} + \frac{1}{\omega_a^e - \omega_s + i\gamma_a} \sum_i \frac{M_i}{\omega_i^e - \omega_L + i\gamma_i^e}, \quad (3)$$

where the summations are over all other allowed intermediate electronic states $|i\rangle$ and $|j\rangle$, which are assumed to be well off resonance, and the M_j and M_i are frequency-independent matrix elements. The first term describes the resonance with the state of energy $\hbar\omega_a^e$ in the incoming channel (in resonance) and the second term describes the resonance with state of energy $\hbar\omega_a^e$ in the outgoing channel (out resonance).

In Cu_2O the 1S "yellow" (1S-Y) exciton at 16 399 cm^{-1} lies almost 1000 cm^{-1} below the next intrinsic electronic state the 2p "yellow" exciton. The width of the 1S exciton is less than 0.2 cm^{-1} at low temperatures,⁴ and thus Raman scattering from the 109- cm^{-1} optical phonon affords an excellent situation for observing both in and out resonance enhancement profiles. Previous work has shown the existence of both in and out resonances and has displayed the unusual polarization asymmetries which characterize the quadrupole-dipole allowed Raman scattering which occurs near this exciton state.^{5,6} However, the shape of the enhancements have not been studied with high-resolution scanning techniques which occurs near this exciton state.^{5,6} However, the shape of the enhancements have not been studied with high-resolution scanning techniques.

The experiment was performed on an unoriented 0.8-mm-thick single crystal (see Ref. 7) of Cu_2O which was mounted in a helium-exchange-gas cell attached to a Janis liquid-helium Dewar. The data were obtained in a back-scattering geometry using

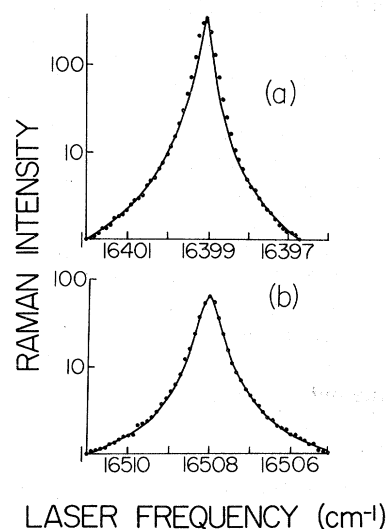


FIG. 1. (a) Resonance Raman enhancement profile for the *in* resonance case. Solid curve is the fit using an exciton damping parameter $\gamma = 0.085 \text{ cm}^{-1}$. (b) Enhancement profile for the *out* resonance. Solid curve uses the same exciton damping as for (a) but includes a phonon damping $\gamma_0 = 0.11 \text{ cm}^{-1}$ as described in the text.

a CRL 490 dye laser with a 0.5-mm etalon for frequency control. For data acquisition the dye laser was stepped in frequency increments of approximately 0.1 cm^{-1} , by rotating the intracavity etalon, while synchronously stepping the Spex 1401 monochromator in identical increments. Spectrometer slit width was 5 cm^{-1} . The laser output, which consisted typically of three distinct cavity modes with a total separation of 0.05 cm^{-1} , was continuously monitored with a Spectra Physics model 470 spectrum analyzer. Laser power variations were automatically compensated by a counting interval normalization system.⁸ High-resolution absorption data was also obtained on the same sample by measuring laser transmission through the sample at normal incidence.

The observed frequency dependence of the cross section for Raman scattering near the 1S-Y exciton in Cu_2O is shown in Fig. 1. Figure 1(a) shows the behavior for the incoming photon resonance and Fig. 1(b) the behavior for the scattered photon resonance. The data have been displayed on a logarithmic scale to permit examination of the wings of the spectra. The solid curves are fits of the spectra to a simple Lorentzian function multiplied by an absorption correction. The fitting function is

$$f(\bar{\nu}) = B(\bar{\nu}) [A / (\bar{\nu} - \bar{\nu}_a)^2 + \gamma^2]. \quad (4)$$

$B(\nu)$ is the absorption correction which for the

in resonance, Fig. 1(a), is given by

$$B(\bar{\nu}) = \frac{\cos \theta}{\alpha(\bar{\nu})} \left[1 - \exp\left(\frac{-\alpha(\bar{\nu})t}{\cos \theta}\right) \right]. \quad (5)$$

θ is the angle of beam propagation in the crystal measured from the surface normal, t is the crystal thickness, and the absorption constant $\alpha(\bar{\nu})$ is directly obtained from our laser absorption data on the same sample. The solid curve in Fig. 1(a) is the fit obtained using the absorption-modified Lorentzian of Eqs. (4) and (5) and yields an exciton width (full width at half-maximum) of $2\gamma = 0.17 \text{ cm}^{-1}$.

For the out resonance case, Fig. 1(b), the absorption correction $B(\nu)$ as a slightly different form since absorption at the incident photon frequencies is negligible and the significant correction occurs for the scattered photon whose frequency is uncertain by an amount γ_0 , the phonon damping. Thus the absorption correction is suitably averaged with a Lorentzian weighting factor of width γ_0 :

$$B(\nu) = \int_{-\infty}^{+\infty} d\bar{\nu}_s \left(\frac{B_0}{(\bar{\nu}_s - \bar{\nu})^2 + \gamma_0^2} \right) \left(\frac{1 - e^{-\alpha(\bar{\nu}_s)t}}{\alpha(\bar{\nu}_s)} \right), \quad (6)$$

where $\bar{\nu} = \bar{\nu}_L - \bar{\nu}_0$ and again $\alpha(\bar{\nu}_s)$ is the measured absorption near the 1S-Y exciton. The solid curve of Fig. 1(b) is the fit to the out resonance data using Eq. (4) with a damping parameter of $2\gamma = 0.41 \text{ cm}^{-1}$ and a phonon width of $2\gamma_0 = 0.24 \text{ cm}^{-1}$ in Eq. (6).

In addition to the slightly different correction for absorption discussed above, the out resonance fit includes a constant background intensity of $9.1 \times 10^{-3} I_0$, where I_0 is the peak Raman intensity. This background signal was directly measured with the laser 10 cm^{-1} off resonance and arises from phonon-assisted absorption via the Γ_{25}^- optical phonon ($\bar{\nu}_0 = 85 \text{ cm}^{-1}$) followed by exciton relaxation and zero phonon luminescence at the 1S-Y exciton line.^{5,9} Because of the weak absorption to this dipole-forbidden exciton, the maximum absorption correction is a factor of 2.6 which occurs at the peak of the in resonance curve where the absorption was measured as $\alpha = 26 \text{ cm}^{-1}$. The correction is negligible more than two half-widths from the peak. Both sets of data show some excess width near the peak but it is particularly apparent in the narrowest data, Fig. 1(a). We interpret this deviation from Lorentzian behavior as arising from inhomogeneous broadening probably related to strains and impurities in the crystal.¹⁰ A Gaussian contribution of width $\sim 0.2 \text{ cm}^{-1}$ will account for these points near the peak but does not change the fit in the wings. For clarity, this

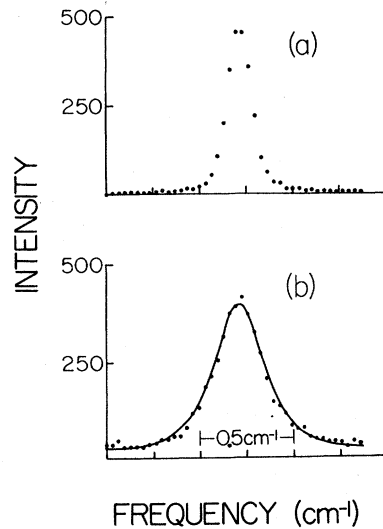


FIG. 2. (a) Instrumental resolution of the Fabry-Perot plus dye laser obtained by scanning the laser line. (b) Observed width of 109 cm^{-1} Raman line. Numerical deconvolution gives a phonon damping of $\gamma_0 = 0.12 \text{ cm}^{-1}$.

Gaussian contribution was not included in the fits of Fig. 1.

To verify that the increased width for the out resonance data is consistent with the phonon-damping contribution, we directly measured the width of the 109-cm^{-1} Raman line when the laser was tuned to the peak of the resonance. The narrow Raman linewidth required the use of interferometric techniques. A Tropel model 360 scanning Fabry-Perot was placed in the collection optics just in front of the double spectrometer. With the spectrometer set to isolate the 109-cm^{-1} Raman line, the Fabry-Perot was repetitively scanned with data collection into a Canberra model 8100 multichannel analyzer. The results of a scan of the dye laser line and the Raman line are shown in Figs. 2(a) and 2(b). Numerically deconvoluting the instrumental linewidth from the observed Raman linewidth yields a true Raman width of 0.22 cm^{-1} .

The estimated uncertainty in the fit to the Fabry-Perot data is $\pm 0.02 \text{ cm}^{-1}$ and for the resonance Raman profiles of Fig. 1 the uncertainty is $\pm 0.01 \text{ cm}^{-1}$ for each curve. Thus the phonon width of $0.22 \pm 0.02 \text{ cm}^{-1}$ obtained by the direct Fabry-Perot determination is consistent with the phonon width of $0.24 \pm 0.02 \text{ cm}^{-1}$ obtained by fitting separately the in and out resonance Raman enhancement profiles. From these results we conclude that the damping parameter appropriate for an out resonance must include both the electronic state damping and the phonon damping in complete agreement

with the theoretical description.

Although for the particular case of Cu_2O both the electronic and phonon widths are unusually narrow, in many situations of interest the phonon widths lie in the range of $1\text{--}10\text{ cm}^{-1}$. In some of these cases, the inclusion of the phonon damping in the terms describing the out resonance may be crucial for an adequate description of resonance Raman scatter-

ing enhancement profiles.

ACKNOWLEDGMENTS

The authors are grateful to Dr. R. A. Forman of the National Bureau of Standards for supplying the Cu_2O crystal. This work was supported in part by the NSF Grant No. DMR 76-00731 and by a Research Corporation Grant.

¹R. Loudon, Proc. R. Soc. Lond. A 275, 218 (1963); J. L. Birman, *Handbuch der Physik*, edited by S. Flügge (Springer-Verlag, Berlin, 1975), Vols. 25 and 26.

²A. Compaan and H. Z. Cummins, Phys. Rev. Lett. 31, 41 (1973).

³M. V. Klein, Phys. Rev. B 8, 919 (1973); R. M. Martin and L. M. Falicov, in *Light Scattering in Solids: Topics in Applied Physics*, edited by M. Cardona, (Springer, New York, 1975), Vol. 8, p. 80.

⁴R. M. Habiger and A. Compaan, Solid State Commun. 26, 533 (1978).

⁵A. Z. Genack, H. Z. Cummins, M. A. Washington, and A. Compaan, Phys. Rev. B 12, 2478 (1975).

⁶J. L. Birman, Solid State Commun. 13, 1189 (1973); Phys. Rev. B 9, 4518 (1974).

⁷Sample preparation is described in A. Compaan, Solid State Commun. 16, 293 (1975).

⁸C. E. Hathaway and L. A. Rahn, Rev. Sci. Instrum. 43, 294 (1972).

⁹P. Y. Yu and Y. R. Shen, Phys. Rev. B 12, 2488 (1975).

¹⁰J. C. Merle, S. Nikitine, and H. Haken, Phys. Status Solidi B 61, 229 (1974).